MODELING AXIAL RELOCATION OF FRAGMENTED FUEL DURING LOSS OF COOLANT CONDITIONS USING THE BISON FUEL PERFORMANCE CODE

K.A. GAMBLE
Fuel Modeling and Simulation, Idaho National Laboratory
P. O. Box 1625, 83415-3840, Idaho Falls – USA

ABSTRACT

Under Loss of Coolant Accident (LOCA) conditions clad ballooning can occur due to internal overpressure and creep in light water reactor fuel rods. Associated with the cladding distension is the possibility of downward relocation of fuel fragments into the distended region of the rod. This axial relocation is of concern because there is the potential of larger amounts of fuel being dispersed if the rod fails. A model has been added to the Bison fuel performance code to take into account the effect of mass relocation on thermal conductivity degradation and heat generation during LOCA events. The mass relocation component of the model has been verified against both single balloon and twin balloon numerical cases for which analytical solutions can be obtained. Validation of the model is underway using integral LOCA tests from the Halden reactor. Verification and validation results are presented.

1. Introduction

Fuel rods subjected to a Loss of Coolant Accident (LOCA) in a nuclear reactor can undergo a complex process known as fuel fragmentation, relocation, and dispersal (FFRD) [1]. The FFRD phenomenon in the fuel is driven by the thermo-mechanical behaviour of the cladding such as ballooning and rupture. In particular, the axial relocation of fuel throughout the rod is of great importance because it causes a redistribution of the heat load within the fuel rod causing further cladding ballooning and ultimately leading to failure and potential dispersal.

In the fuel performance modeling community limited models exist to predict the axial relocation behavior of fuel during a LOCA. This paper reviews the literature for axial relocation modeling and describes the implementation of one of the models into the Bison fuel performance code [2] developed at Idaho National Laboratory (INL). Verification of the mass relocation portion of the algorithm is presented using examples for which analytical solutions can be obtained. Preliminary validation of the algorithm to the Halden IFA-650.9 LOCA test is also provided.

2. Theory

The axial movement of fuel during a LOCA is influenced by many factors including the size of fuel fragments formed during irradiation and the amount of cladding distension. It should be noted that this phenomenon has been observed experimentally (See Fig.1). In this neutron radiograph one observes that some intact fuel remains above the voided region (right side of the radiograph). This is because the cladding has not distended enough to release the fuel in this region.

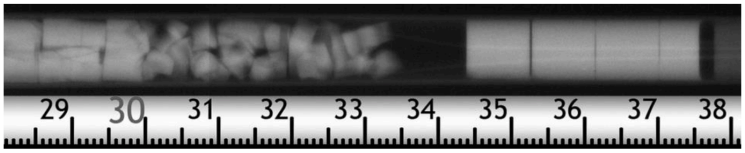

Fig. 1: Neutron radiograph illustrating fuel axial relocation. Figure reproduced from [1].

Currently in the literature there exists two models that have been developed in an attempt to predict fuel axial relocation in fuel performance codes. The first by Siefken [3] was developed based upon analysis of two experimental LOCA test series completed at the Power Burst Facility in the United States and the FR2 reactor in Germany. Siefken proposed that the fuel at one axial location would translate to another if the void fraction exceeded a critical value of 0.30. The void fraction represents the amount of space within the clad at the axial location that does not comprise of fuel. In a particular axial layer, *z*, the void fraction is calculated by:

$$\alpha_z = 1 - \frac{V_{fz}}{V_{cz}} \tag{1}$$

where α_z is the void fraction, V_{fz} is the fuel volume per unit length, and V_{cz} is the inner cladding volume per unit length. In layers deemed to exceed the critical value for void fraction the radial heat transfer calculation is updated to take into account the redistribution of the fuel. Unfortunately, Siefken's model assumes constant void fraction independent of fuel fragmentation size and is based upon limited experiments up to burnups of only 35 MWd/kgU.

Building upon the knowledge gained over approximately 30 years since the previous model Jernkvist and Massih [4] proposed a more sophisticated axial relocation model to wrap around the fuel performance code FRAPTRAN-1.5. FRAPTRAN-1.5 utilizes a layered 1D approach for modeling the fuel rod. In a layered 1D analysis the fuel rod is divided into a number of axial layers, each of which is represented using a 1D axisymmetric model with generalized plane strain assumptions. These simulations are solved using a finite difference technique in FRAPTRAN.

The model proposed is more sophisticated than Siefken's because it allows for the packing fraction (ϕ), which is equivalent to $(1-\alpha)$ to evolve depending upon the irradiation of the fuel. The packing fraction is calculated assuming a binary system of particle sizes that is used to differentiate fuel fragments formed during normal irradiation (fragments) and those that form in high burnup fuel through a process known as pulverization (pulvers). This is the model implemented into the Bison code for axial relocation modeling.

In the Bison implementation the correlation used for determining the size of fragments is the model proposed by Coindreau et al. [5] which calculates the number of fragments in fresh fuel before including irradiation (burnup) effects through:

$$n_f^o = \max\left(1, \min\left(\frac{7.0\, q'_{\max} - 8.0}{17.0}\right), 16.0\right) \tag{2a}$$

$$n_f = \min\left(n_f^o + \frac{\left(16.0 - n_f^o\right) Bu_{av}}{50.0}, 16.0\right) \tag{2b}$$

where n_f^o is the number of radial fragments expected in fresh fuel subjected to the maximum power experienced by the fuel, $q'_{\max}$ in kW/m, and n_f is the total number of fragments expected taking into account the average burnup of the fuel rod given by Bu_{av} in MWd/kgHM. Once the number of fragments is known the characteristic length of the fragments is calculated via:

$$l_f = D_{FP} \min\left(1, \frac{\pi}{n_f}\right) \tag{3}$$

where l_f is the characteristic length in m and D_{FP} is the fuel pellet diameter in m. Limited experimental data exists for the size of fuel particles formed during pulverization. Pulverization of the fuel is hypothesized to be caused by overpressurization of gas bubbles in the highly porous high burnup structure that forms at the pellet periphery as irradiation progresses. The

overpressurization and rupture of these bubbles results in the porous region of fuel disintegrating into very fine particles. Turnbull et al. [6] have developed a pulverization threshold that is a local temperature function of local burnup as shown in Fig. 2. Jernkvist and Massih argue that even if the threshold has been exceeded and there is a contact pressure between the fuel and cladding of greater than 50 MPa pulverization will not occur. Additional validation of the pulverization threshold beyond the experiments upon which it was developed and discussed by Turnbull et al. [6] has not been completed.

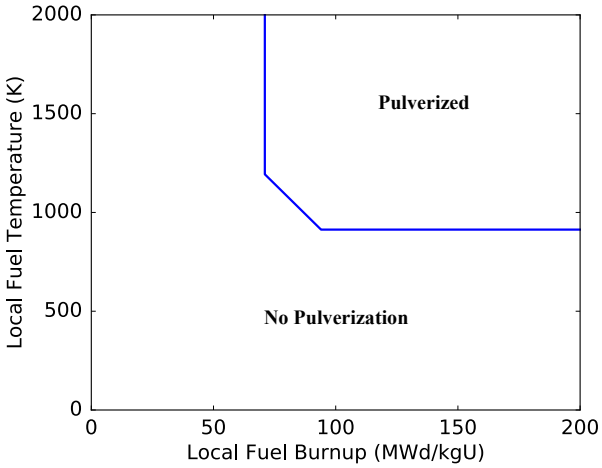

Fig. 2: Burnup dependent temperature threshold for pulverization of UO_2 fuel.

Once the volume of the pellet subjected to pulverization in a layer is determined the mass fraction of pulverized fuel (x_p) is calculated knowing the total volume of fuel in a particular layer (in the layered 1D modeling approach). The mass fraction of fragments (x_f) is simply given by $x_f = 1 - x_p$. Given the known mass fractions the packing fraction can be calculated by solving the following set of equations using an internal newton solve to iterate to convergence within a specified tolerance.

$$a^2 + 2Gab + b^2 = 1.0 \tag{4a}$$

$$a = \frac{\phi_p(\phi_f - x_f\phi)}{\phi\phi_f} \tag{4b}$$

$$b = \frac{\phi_p\phi_f - \phi\phi_f(x_p + x_f\phi_p)}{\phi\phi_p(1 - \phi_f)} \tag{4c}$$

$$G = \begin{cases} 0.738\left(D_p^p/D_p^f\right)^{-1.566}, & D_p^p/D_p^f \le 0.824 \\ 1.0, & D_p^p/D_p^f > 0.824 \end{cases} \tag{4d}$$

$$D_p = \left(3.9431 - \frac{4.5684}{\psi} + \frac{1.8660}{\psi^2}\right) V_p^{1/3} \tag{4e}$$

where a, b, and G are unitless parameters, ϕ_p (default value of 0.72) and ϕ_f (default value of 0.69) are the packing fractions assuming the crumbled bed of fuel particles is entirely made up of pulvers or fragments respectively, ϕ is the packing fraction of the binary system (what is being solved for), D_p^p and D_p^f are the equivalent packing diameters of the pulvers and fragments, and ψ and V_p are the sphericity and volume of a particular particle shape. Jernkvist and Massih suggest that fragments are treated as prismatic and pulvers as octahedral. Thus,

for fragments, $\psi = 0.716$ and $V_p = 0.4330 l_f^2$ where l_f is the characteristic length calculated from Equation 3. For pulvers, $\psi = 0.846$ and $V_p = 0.4714 l_p^3$ where l_p is the characteristic length of the pulver (default value of 100 μm).

Once the packing fraction is obtained the rest of the axial relocation algorithm can be completed including mass relocation, thermal conductivity degradation, increase of effective diameter of the porous bed of fragments in layers that have crumbled for heat redistribution, and internal volume calculations upon fuel crumbling. The condition on fuel crumbling in a given layer is given by

$$m_k^M > m_k^i \tag{5}$$

where m_k^i represents the initial mass in the k:th layer and m_k^M represents the mass in the layer if it is completely filled with crumbled fuel given by

$$m_k^M = \phi_k \rho_f \pi L_k R_{cik}^2 \tag{6}$$

where ϕ_k is the packing fraction for the k:th layer, ρ_f is the fuel density, L_k is the length of the k:th layer and R_{cik} is the inner cladding radius in the k:th layer. In addition to the condition of crumbling four additional constraints are required for realistic and numerical reasons. The first two constraints prevent fuel from relocating upwards within the fuel rod and limit the amount of fuel that can relocate to the total amount of existing mass in layers above a given layer. These lower (m_k^L) and upper (m_k^U) mass constraints are given by

$$m_k^L = \sum_{j=1}^{k} m_j^o - \sum_{j=1}^{k-1} m_j \tag{7a}$$

$$m_k^U = m_k^r + m_k^L \tag{7b}$$

where the m_j^o represents the mass in the j:th layer at the beginning of the timestep (t_o), m_j represents the current mass in the j:th layer and m_k^r represents the available mass to be relocated into the k:th layer. The two other constraints assume a small fraction of the initial fuel mass in a layer will remain in that layer (i.e., stuck to the cladding) which is denoted by x^r with a default value of 0.01 and the cladding distention must be sufficiently large in a layer to generate a fuel-to-cladding gap that will accommodate fuel movement (denoted by g^{th} with a default value of 0.2 mm). The mass relocation algorithm given the above definitions and constraints is divided into two loops. The first loop iterates from the top of the fuel rod downward determining the amount of fuel that can be relocated into a particular layer. The second updates the mass in the layers while enforcing the lower and upper constraints by iterating from the bottom of the rod upward. These loops have been modified for clarity from [4] and are illustrated in Fig. 3 and Fig. 4. These loops verified with two examples in the verification subsection of this paper.

In layered 1D modeling approaches only the radial component of the heat equation is solved. As layers crumble the effective diameter of the fuel needs to change to resemble pointwise contact with the cladding. In the Bison implementation this movement of the mesh is achieved by applying a fictitious eigenstrain that radially moves the mesh. This is an acceptable approach given that once crumbled calculating the stress state correctly is not necessary within the fuel. The modified heat equation is given by

$$\phi \rho_f c_{pf} \frac{\partial T}{\partial t} - \frac{1}{r'} \frac{\partial}{\partial r'} \left(k_{eff} r' \frac{\partial T}{\partial r'} \right) = \phi q''' \tag{8}$$

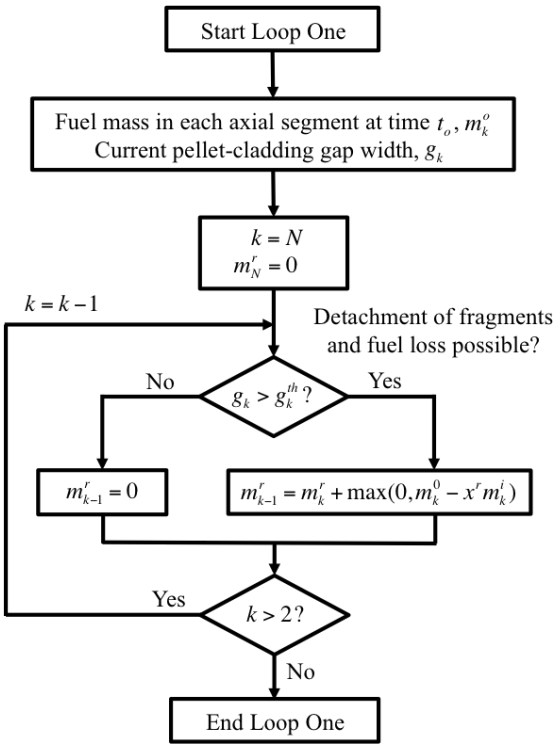

Fig. 3: The first loop of the axial relocation algorithm which determines the amount of relocatable mass m^r that can be accommodated in each layer.

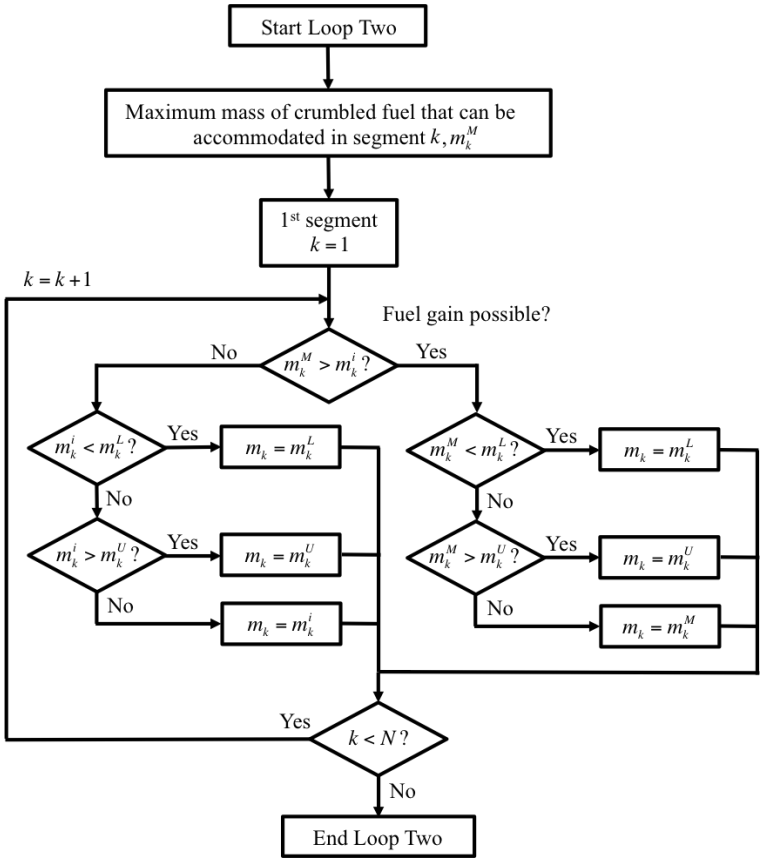

Fig. 4: The second loop of the axial relocation algorithm that enforces the constraints and moves the mass to the appropriate layers.

Where c_{pf} is the specific heat capacity of the fuel, r' is the modified radial coordinate system, k_{eff} is the effective thermal conductivity of crumbled fuel and gas mixture, and q''' is the volumetric heat generation rate. In layers partially or completely void of the fuel, the original radial position is used along with the fuel thermal conductivity instead of k_{eff}. The volume of these layers is scaled to account for the mass loss in rod internal pressure calculations. The correlation used to calculate k_{eff} is that by Chiew and Glandt [7].

3. Verification and Validation

With any new model added to the Bison fuel performance code it must be verified and validated. Verification comes in two flavours, solution and code. Solution verification ensures that the mesh and timesteps used are sufficiently resolved to calculate a consistent solution. Code verification ensures that the coded model behaves as expected when comparing to an analytical or known numerical solution. Validation on the other hand is comparison of the model to reality (i.e., experiments). In this paper two verification cases are presented, and a single validation case is explored.

3.1 Verification Cases

Jernkvist and Massih [4] developed two simplistic cases to test the implementation of the axial relocation algorithm loops that determine the amount of relocatable mass and updates the mass given the upper and lower mass constraints. The implementation of the algorithm in Bison was compared to the results obtained by Jernkvist and Massih for these two simplistic cases for verification purposes.

The two cases considered are referred to as a single balloon and twin balloon respectively. In both test cases the active fuel length is 3.6 m with a fuel pellet diameter of 9.0 mm. The initial fuel-to-cladding gap is assumed to be zero (i.e., the gap is closed). The packing fraction is assumed to be 0.75 after fuel crumbling in each layer and 36 equal length axial segments are used. The duration of the simulation is 100 s. The single balloon verification test is to simulate cladding distention that is maximum at the midplane of the active length (z = 1.8 m). The twin balloon verification test is to simulate the effect of having a spacer-grid at the midplane of the active length.

In the single balloon test the inner cladding radius is varied as a function of time and axial position as follows:

$$R_{ci}(t,z) = 4.5 \times 10^{-3} + 2.0 \times 10^{-5} t \sin\left(\frac{\pi z}{L_a}\right) \tag{9}$$

and in the twin balloon test the inner cladding radius is varied via:

$$R_{ci}(t,z) = 4.5 \times 10^{-3} + 2.0 \times 10^{-5} t \left|\sin\left(\frac{2\pi z}{L_a}\right)\right| \tag{10}$$

where R_{ci} is the cladding inner radius in m, z is the axial position from the bottom of the active fuel in m, t is the time in seconds, and L_a is the active fuel length in m. The Bison results of these test cases are compared to the digitized results from the Jernkvist and Massih [4] report in Fig. 5. Three panels are shown for each case representing different times through the duration of the simulation corresponding to 40, 60, and 100 s. The plots show the mass fraction of fuel as a function of axial position. A mass fraction >1 indicates that mass has accumulated in this region and a mass fraction <1 corresponds to a region partially (or completely) void of fuel. As expected in the regions near the maximum cladding ballooning the mass fractions are largest. It should be noted that at the very top of the fuel rod the mass fraction remains as 1. This is because the cladding distention would never be large enough in this top layer to allow fuel to relocate out of it. This behavior is observed experimentally (See Fig. 1). As is evident

in both verification test cases, the Bison implementation has been verified to be correct as the results match Jernkvist and Massih's results extremely well.

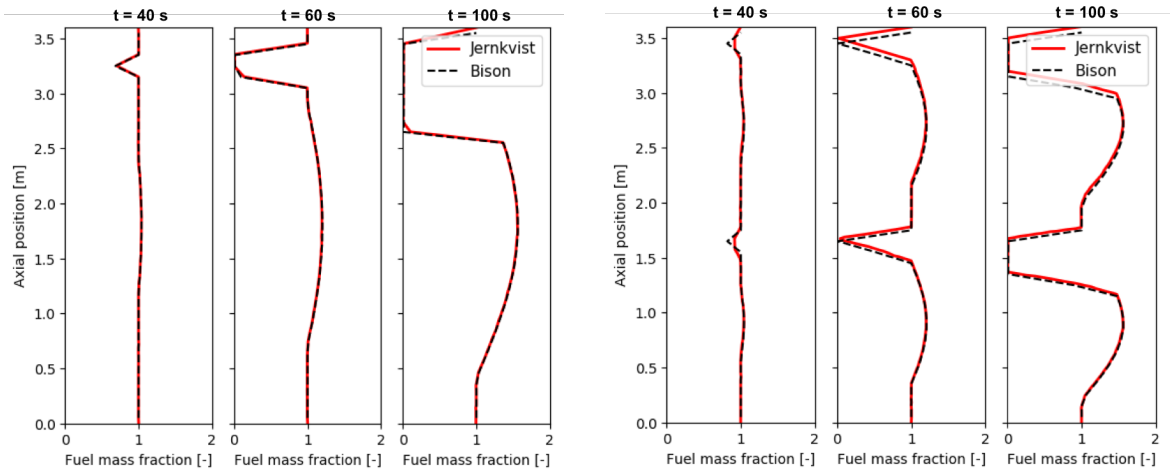

Fig. 5: Comparisons between the Bison predictions and the presented results of Jernkvist and Massih for the fuel mass fraction as a function of axial position at select snapshots in time for single balloon (left) and twin balloon (right).

3.2 Halden Case IFA-650.9

As mentioned previously, validation is the comparison of the implemented model to experiments. The Instrumented Fuel Assembly (IFA)-650 series of experiments completed at the Halden Reactor in Norway have been designed to investigate fuel behavior under a variety of LOCA conditions. A few were observed to experience axial fuel relocation. In this paper the preliminary results of the IFA-650.9 experimental test compared to the model predictions to the Bison code are presented.

The IFA-650.9 experiment was used to measure the cladding temperature, rod internal pressure and clad elongation during a LOCA transient on highly irradiated fuel. Fuel relocation was also observed. The experiment was conducted on a small subsection of a previously commercially irradiated mother rod from the Swiss NPP Gösgen up to an average burnup of 89.9 MWd/kgU. During the test the rodlet has minimal power supplied to the fuel with additional heating to the cladding surface through a heater. Following refabrication the rodlet was subjected to a conditioning phase for nuclear power calibration prior to the LOCA. After the conditioning phase the rodlet was subjected to five phases: blowdown, ballooning, burst, spray (rewet), and scram. In the Bison analyses the simulation was terminated when the code predicted burst. Burst was predicted in the experiment to occur at 133 seconds [8].

The difficulty in performing a fuel performance analysis of a LOCA experiment is the difficulties in capturing the cladding surface temperature or coolant boundary conditions correctly. To this end, the internal Bison coolant channel model is used for the base irradiation to calculate the fuel to cladding heat transfer coefficient. During the preconditioning phase the measured cladding temperatures are directly applied to the cladding surface because if the rod is not properly preconditioned there is no hope in having reasonable predictions during the transient. At the onset of the blowdown phase the coolant channel model is turned back on with the option to model radiative heat transfer in addition to the convective component. Thirty axial layers were used to model the fuel stack and a single layer for the plenum region.

The Bison simulation covers all of the phases of the rodlets life including the base irradiation, preparatory, blowdown, and heat up phases up to the point of failure of the fuel rod cladding.

Results for fuel relocation (mass fraction), cladding profilometry, and rod internal pressure are presented. According to Di Marcello et al. [10] the failure criterion to be used during large strain analyses such as the one analyzed here is not unique given the large amount of uncertainty in the experimental conditions. Therefore, two different failure criteria were used and compared to available experimental data for the IFA-650.9 rodlet. These criteria are known as the plasticity instability limit and the overstrain limit. In the plastic instability criterion, the cladding is said to have failed when its outer surface experiences an inelastic strain rate of 2.778×10^{-2} s^{-1}. In the overstrain criterion the cladding is said to have failed when the average permanent tangential (hoop) strain (i.e., from creep) exceeds an engineering strain value of 40% or a true strain (as used in Bison) of 33.6%. In the subsequent results plots the simulations utilizing the different failure criteria are denoted by PI (plastic instability) and OS (overstrain), respectively.

As the cladding balloons during the blowdown and heat-up phases the highly fragmented fuel (due to irradiation to high burnup in the commercial reactor) may be permitted to relocate from upper portions of the rodlet into the ballooned region(s). As the mass relocates the effective diameter of the fuel in the model should be moved radially almost into contact with the cladding to simulate point-wise contact and for thermal feedback purposes resulting in further localized ballooning to the point of failure. This modified radial coordinate position is denoted by r' in Equation 8. Depending on the failure criterion used the time to burst is vastly different. The predicted time to burst by the Bison simulations were 111.3 s and 115.1 s for the plastic instability and overstrain cases, respectively. The measured value was ~133 s.

Comparisons of the Bison simulations to the experimental data are shown in Fig. 6. The left plot shows the outer cladding diameter profilometry at the time of burst (i.e., end of the simulation) compared to the measured profilometry at the end of the LOCA transient. No uncertainty on the experimental cladding diameter measurements were provided in the available documentation for the experiment. As expected, the cladding profilometry follows a similar trend as the fuel mass fraction predictions (see right figure) because the fuel movement is directly a function of the cladding distention. Therefore, at the location of the largest mass fraction is also the location of the largest cladding diameter predictions. The Bison simulations more accurately capture the midplane balloon (at least by the overstrain criterion) but not the experimentally measured burst balloon at the bottom of the rod. The simulated cladding diameters extend to a larger axial position due to the increased plenum length required to achieve the free volume fabricated into the experimental rig. The right figure illustrates the fuel mass fraction as a function of axial position captured by the model at the time of burst compared to a gamma scan of ^{137}Cs that took place 6 weeks after the conclusion of the experiment. A higher cesium concentration indicates more mass is present in the region. The Bison simulations indicate that for the plastic instability criterion that failure occurs before mass can relocate whereas for the overstrain criterion mass accumulates in the midplane region of the rodlet which coincides with the increased gamma scan reading at that location. However, the Bison simulations fail to predict the large ballooning and rupture location at the bottom of the rodlet. However, the Bison results are taken at the time of burst whereas the gamma scan is taken 6 weeks after the termination of the experiment where handling and transport of the rodlet for PIE could also affect the redistribution of the fuel as the rodlet is handled during PI causing further axial movement. In addition, the model assumes instantaneous relocation of the fuel to satisfy equilibrium packing. There is a possibility that additional relocation could be induced by the pressure decrease after burst which is not captured by the Bison simulations. The fuel mass fraction of 1.0 at the very top of the rod is expected given that the cladding has not distended enough at this location to permit fuel movement.

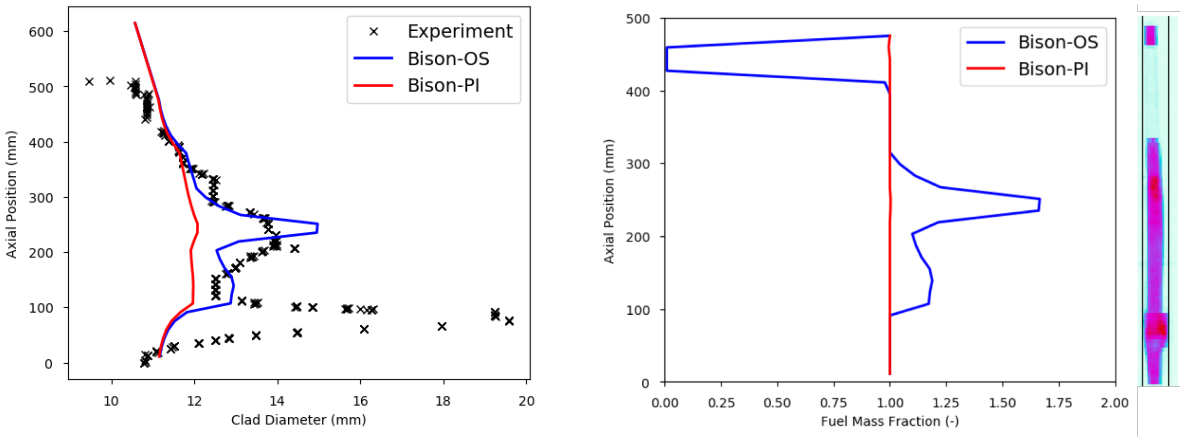

Fig. 6: Comparison to experiment (obtained data package included with [8]) from for cladding diameter (left) and predicted mass fraction as a function of axial position within the fuel stack at time of burst (right).

4. Conclusions

A sophisticated axial relocation model developed by Jernkvist and Massih [4] has been added to the Bison fuel performance code. The details of the mass relocation portion of the algorithm have been summarized and the implementation has been verified through comparisons to single and twin balloon cases. Initial validation has been completed against the IFA-650.9 Halden experiment. The predicted time to burst was underpredicted relative to the experiment (~133 s) with the plastic instability criterion resulting in a rupture prediction of 111.3 s and the overstrain criterion predicting rupture at 115.1 s. The discrepancy between the time predictions is due to a larger calculated rod internal pressure than experimentally observed. The central balloon was adequately captured by the Bison simulations whereas the large balloon at the bottom of the fuel rod was not. Mass was observed to move into the ballooned region at the center of the rod. An investigation into why the calculated internal pressures are larger than in the experiment is required to improve the burst time predictions.

5. Future Work

The IFA-650.9 experiment was only one of multiple experiments in the IFA-650 series that experienced axial fuel relocation. Further validation of the model can be accomplished by simulating these additional experiments including IFA-650.4, IFA-650.10, and IFA-650.14. In addition, the axial relocation algorithm is built upon a layered 1D framework which assumes azimuthal symmetry. Many of these LOCA experiments provide azimuthal variation in cladding temperature measurements which would be important to capture. Therefore, the axial relocation model needs to be extended to 2D or 3D to allow azimuthal variations in temperature.

6. Acknowledgements

This work was funded by the U.S. Department of Energy under the Consortium for Advanced Simulation of Light Water Reactors (CASL). The conference paper has been authored by a contractor of the U.S. Government under Contract DE-AC07-05ID14517. Accordingly, the U.S. Government retains a non-exclusive, royalty free license to publish or reproduce the published form of this contribution, or allow others to do so, for U.S. Government purposes.

7. References

[1] H. Sonnenburg, W. Wiesenack, J. Karlsson, J. Noirot, V. Garat, N. Waeckel, F. Khattout, A. Cabrera-Salcedo, J. Zhang, G. Khvostov, A. Gorzel, V. Brankov, F. Nagase, P. Raynaud, M. Bales, T. Taurines, T. Nakajima, and A. Alvestav, *"Report on fuel fragmentation, relocation, and dispersal,"* Tech. Report NEA/CSNI/R(2016)16, Organisation for Economic Co-operation and Development, Nuclear Energy Agency, Committee on the Safety of Nuclear Installations, 2016.

[2] R. L. Williamson, K. A. Gamble, D. M. Perez, S. R. Novascone, G. Pastore, R. J. Gardner, J. D. Hales, W. Liu, and A. Mai, "*Validating the BISON fuel performance code to LWR experiments*," Journal of Nuclear Materials **301** (2016), pp. 232-244.

[3] L. J. Siefken, *"Fuel axial relocation in ballooning fuel rods*," International Conference on Structural Mechanics in Reactor Technology, Chicago,1983.

[4] L. O. Jernkvist and A. Massih, *"Models for axial relocation of fragmented and pulverized fuel pellets in distending fuel rods and its effects on fuel rod heat load,*" Tech. Report 2015:37, Quantum Technologies AB, 2015.

[5] O. Coindreau, F. Fichot, and J. Fleurot, *"Nuclear fuel rod fragmentation under accidental conditions,"* Nuclear Engineering and Design **255** (2013), pp. 68-76.

[6] J. A. Turnbull, S. K. Yagnik, M. Hirai, D. M. Staicu, and C. T. Walker, *"An assessment of the fuel pulverization threshold during LOCA-type temperature transients,"* Nuclear Science and Engineering **179** (2015), pp. 477-485.

[7] Y. C. Chiew and E. D. Glandt, *"The effect of structure on the conductivity of a dispersion,"* Journal of Colloid and Interface Science **91** (1983), no. 1, pp. 90-104.

[8] F. Bole du Chomont, *"LOCA Testing at Halden, the Ninth Experiment IFA-650.9."* Tech. Report HWR-917, OECD Halden Reactor Project, 2009.

[9] L. O. Jernkvist and A. Massih, *"Modelling axial relocation of fragmented fuel pellets inside ballooned cladding tubes and its effects on LWR fuel rod failure behavior during LOCA,*" Transaction of SMirT-23, Manchester UK, 2015.

[10] V. Di Marcello, A. Schubert, J. van de Laar, and P. Van Uffelen, "*The TRANSURANUS mechanical model for large strain analysis,"* Nuclear Engineering and Design, **276** (2014), pp. 19-29.